

Creation of a Nanoskyrmion Lattice in the Fe/Ir(111) System Using a Voltage Pulse

Yulong Yang^①,¹ Mingming Shuai,¹ Haiming Huang,¹ Rui Song,¹ Yi Zhu,¹ Yanghui Liao,¹ Yinyan Zhu,^{1,2,3} Xiaodong Zhou^{②,*,†},^{1,2,3,4,5}, Lifeng Yin^{③,1,2,3,4,5,†}, and Jian Shen^{1,2,3,4,5,‡}

¹State Key Laboratory of Surface Physics, Institute for Nanoelectronic Devices and Quantum Computing, and Department of Physics, Fudan University, Shanghai 200433, China

²Shanghai Qi Zhi Institute, Shanghai 200232, China

³Zhangjiang Fudan International Innovation Center, Fudan University, Shanghai 201210, China

⁴Shanghai Research Center for Quantum Sciences, Shanghai 201315, China

⁵Collaborative Innovation Center of Advanced Microstructures, Nanjing 210093, China

(Received 1 March 2023; revised 6 May 2023; accepted 6 June 2023; published 30 June 2023)

Magnetic ultrathin films grown on heavy metal substrates often exhibit rich spin structures due to the competition between various magnetic interactions such as Heisenberg exchange, Dzyaloshinskii-Moriya interaction and higher-order spin interactions. Here we employ spin-polarized scanning tunneling microscopy to study magnetic nanoskyrmion phase in Fe monolayer grown on Ir(111) substrate. Our observations show that the formation of nanoskyrmion lattice in the Fe/Ir(111) system depends sensitively on the growth conditions and various nonskyrmion spin states can be formed. Remarkably, the application of voltage pulses between the tip and the sample can trigger a nonskyrmion-to-skyrmion phase transition. Such a phase transition is determined by the total injected energy during the voltage pulse suggesting that there exists a potential barrier between a metastable nonskyrmion spin state and a true skyrmion ground state. The creation of a skyrmion lattice at the nanoscale will be useful to design skyrmion-based spintronic devices.

DOI: 10.1103/PhysRevApplied.19.064088

I. INTRODUCTION

Magnetic ultrathin films grown on heavy metal substrates have been a fruitful playground to study magnetism in reduced dimensions [1,2]. The magnetic ground state of such a seemingly simple system turns out to be complex as it is determined by various magnetic interactions, such as Heisenberg exchange, Dzyaloshinskii-Moriya interaction (DMI), and even higher-order spin interactions. If the Heisenberg exchange dominates, collinear ferromagnetic (FM) or antiferromagnetic states are formed. When the DMI becomes comparable to the exchange interaction, various noncollinear spin states can form [3–6]. The competition between various magnetic interactions is pronounced in Fe/Ir(111) ultrathin film system, where the hybridization between the $3d$ state of Fe and the $5d$ state of Ir suppresses the Heisenberg exchange interaction in the Fe layer enabling spin interactions of higher order to play a crucial role in determining the magnetic ground state of the system. It has been experimentally observed that Fe islands

with monolayer thickness are in a magnetic nanoskyrmion state [7–12], and Fe islands with bilayer or trilayer thickness are in a spin-spiral state [13,14]. A recent experiment further indicates that the formation of the nanoskyrmion state is strongly influenced by the Fe adatom diffusion rate during the growth [15]. The nanoskyrmion state exists only in Fe monolayer islands with a perfect triangular shape. In other words, different nonskyrmion spin states may exist in Fe monolayer islands on Ir(111) substrate that compete with the nanoskyrmion state.

Magnetic skyrmion can be utilized as the information bits in future spintronic devices, for which an electrical manipulation of skyrmion (creation, annihilation, and movement) is essential for its integration into modern electronic technology [16–22]. An early study of the Pd/Fe bilayer on Ir(111) showed that individual skyrmion can be written and deleted in a controlled way by local spin-polarized currents from a scanning tunneling microscopy (STM) tip [23,24]. Considering the high-energy dissipation and the Joule heating in such an electric current involved operation, a pure electric field method is called for to achieve the low-energy consumption. This was later realized in another STM study, in which an individual magnetic skyrmion in a trilayer Fe island on Ir(111) can

*zhouxd@fudan.edu.cn

†lifengyin@fudan.edu.cn

‡shenj5494@fudan.edu.cn

be switched reversibly from the skyrmion state to the FM state by a tip induced local electric field [14]. These experiments demonstrate that the Fe/Ir(111) system is a fertile playground for exploring the electrical manipulation of skyrmion. It is noted that the skyrmion phase in the aforementioned works exist only under an external magnetic field. In this regard, the Fe monolayer on Ir(111) is unique as it exhibits a skyrmion phase at zero field, which is also beneficial for the application. Therefore, it would be interesting to investigate the Fe monolayer on Ir(111) and see if its skyrmion phase can be electronically manipulated.

In this work, we report the use of a voltage pulse from a STM tip to transit a nonskyrmion metastable spin state to the magnetic nanoskyrmion state in Fe monolayer islands on Ir(111) substrate. Once formed, the skyrmion phase remains unchanged upon further applications of voltage pulses, indicating that the skyrmion state is likely a true ground state in the Fe monolayer islands on Ir(111).

II. RESULTS AND DISCUSSION

Fe is thermally deposited with a nominal thickness of submonolayer on an Ir(111) single-crystal surface. Prior to the Fe deposition, the Ir(111) single crystal is prepared by cycles of Ar^+ ion sputtering and annealing at $T = 1500$ K. It is further annealed at oxygen atmosphere (2×10^{-6} mbar) at a slightly lower temperature (1200 – 1400 K) to get rid of the surface impurities, which is crucial to obtain the skyrmion lattice [15]. Fe is evaporated from a rod heated by an *e*-beam bombardment. The deposition is conducted when the substrate is at room temperature. A bulk Fe tip with 0.25 mm in diameter is used in the STM measurement, whose magnetic moment at the tip apex points along its axis resulting in a sensitivity to

the out-of-plane component of the sample magnetization. This spin-polarized STM (SPSTM) enables us to resolve the magnetic structure in real space at the atomic scale [25]. All SPSTM experiments are performed at 5 K in the absence of any external magnetic field.

Figure 1(a) shows a SPSTM constant-current image of typical Fe islands grown on an Ir(111) substrate. Two triangular-shaped monolayer islands point in opposite directions, corresponding to fcc and hcp stackings, respectively. An island formed by second-layer Fe adatoms is observed in the middle of the fcc island. A differentiated image of Fig. 1(a) is displayed in Fig. 1(b) for a better visualization of the signal contrast. In the fcc island, a square lattice is observed in the monolayer region, which is known as the magnetic nanoskyrmion state [7–9]. Its magnetic origin is confirmed by a field-dependent measurement (see Appendix A). This nanoskyrmion lattice has multiple domains with different orientations [denoted by the green arrows in Fig. 1(b)] because its fourfold symmetry is different from the threefold symmetry of the underlying hexagonal atomic lattice of Fe/Ir(111). The hcp island displays another nanoskyrmion state with a hexagonal lattice [26]. The nanoskyrmion phase is totally absent in the bilayer region where reconstruction lines along three different orientations are observed. It is a spin spiral state according to previous studies [13,14].

In addition to the aforementioned results consistent with previous reports, we have other observations in the Fe monolayer islands on Ir(111). Figure 1(c) shows a SPSTM constant-current image of a different fcc Fe monolayer island. Compared to Fig. 1(a), we modify the color scheme of Fig. 1(c) to enhance the relatively weak signal contrast on the island. A similar color scheme is adopted in other SPSTM constant-current images of this

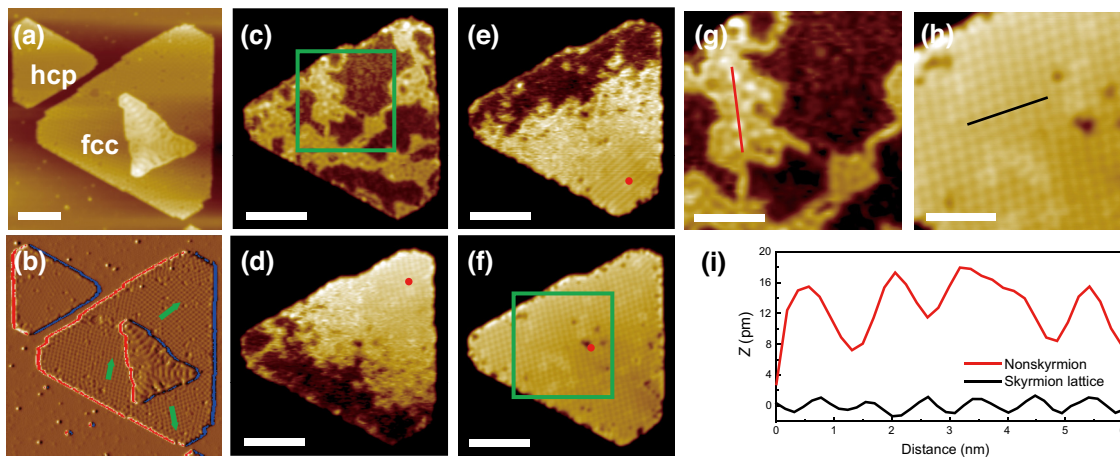


FIG. 1. (a),(b) SPSTM constant-current image and the corresponding differentiated image of Fe monolayer and double layer grown on an Ir(111) substrate ($U = 50$ mV, $I = 100$ pA). (c)–(f) SPSTM constant-current images of an fcc stacking Fe monolayer island subjected to different tip voltage pulses. $U = 50$ mV, $I = 100$ pA for (c) and $U = 100$ mV, $I = 200$ pA for (d)–(f). (g),(h) Close-up images of the square areas denoted in (c),(f). (i) Line-up height profiles of the nonskyrmion and skyrmion lattice phase. The scale bar for (a)–(f) is 10 nm and for (g),(h) is 5 nm.

paper whenever applicable. Figure 1(c) displays a spatial coexistence of “bright” and “dark” regions without the regular nanoskyrmion lattice. Instead, one sees a small labyrinthine pattern in the “dark” region, and a bubble pattern in the “bright” region. To simplify the data description and discussions hereafter, we refer to the states without a clear skyrmion lattice as a nonskyrmion phase. Strikingly, we observe that the nonskyrmion phase can be transited to the skyrmion phase by a tip voltage pulse across the STM tip-sample tunneling junction. Figure 1(d) show a SPSTM constant-current image of the same Fe island after the application of a +6 V voltage pulse (50 ms duration, sample is positive while the tip is grounded) to the upper-right corner of the island [red circle in Fig. 1(d)]. A regular skyrmion lattice is formed in regions surrounding the voltage-pulse location. The rest areas closer to the lower-left edge of the island remains in the nonskyrmion phase. A second voltage pulse is then applied to lower-right corner of the island as shown in Fig. 1(e). After the second voltage pulse, the island rearranges its spin states by rotating the pattern clockwise from the upper-right corner to the lower-right corner. The skyrmion lattice also “moves” to the lower-right corner accordingly. While the nonskyrmion-to-skyrmion phase transition occurs in regions near the voltage-pulse location under the +6 V voltage pulse, the whole island can be converted into a clean and uniform skyrmion phase by applying a higher voltage pulse (+8 V, 50 ms duration) to its center [Fig. 1(f)]. Interestingly, this tip voltage-pulse-induced skyrmion lattice displays only a single domain with one orientation, different from the multidomain state, which is often observed in the as-grown Fe islands [e.g., Figs. 1(a) and 1(b)]. This is a clear indication that the tip voltage-pulse-induced skyrmion lattice is formed by nucleation and growth of a single skyrmion domain while an as-grown Fe island may host skyrmion domains nucleated from different regions of the island.

To closely compare the nonskyrmion phase to the skyrmion phase before and after the tip voltage pulse, Figs. 1(g) and 1(h) show two close-up images of areas denoted in Figs. 1(c) and 1(f), respectively. Figure 1(i) shows the height profile along a selected line in Figs. 1(g) and 1(h). Unlike the skyrmion square lattice with a periodicity of 1 nm, the bubble pattern in the nonskyrmion phase displays a less regular and larger periodicity suggesting its nonskyrmion origin.

The tip voltage-pulse-induced nonskyrmion-to-skyrmion phase transition occurs not only in fcc Fe islands, but also in hcp Fe islands and in Fe strips grown along the Ir(111) substrate step edge. Figure 2 shows a large sample area across an Ir(111) substrate step edge before [Figs. 2(a)–2(c)] and after [Figs. 2(d)–2(f)] multiple tip voltage pulses (+8 V, 50 ms duration). Both fcc and hcp Fe monolayer islands exist, together with a Fe strip along the Ir(111) step edge. While a clear skyrmion lattice cannot be observed in the as-grown state of these Fe areas [Figs. 2(a)

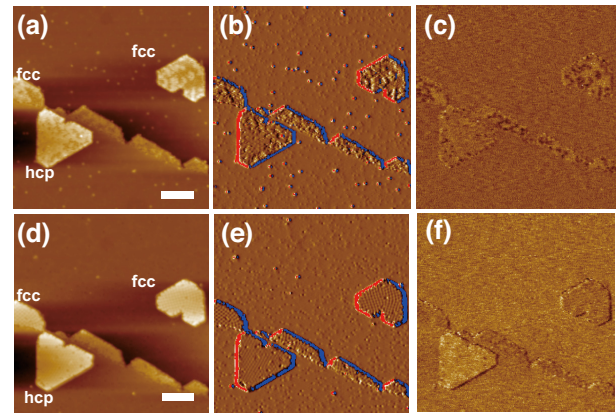


FIG. 2. (a)–(c) SPSTM constant-current image, the differentiated image and the dI/dU map of a large sample area before the application of a tip voltage pulse. (d)–(f) SPSTM constant-current image, the differentiated image and the dI/dU map of a large sample area after the application of a tip voltage pulse. $U = 50$ mV, $I = 200$ pA for all and the scale bar is 10 nm.

and 2(b)], it appears after the tip voltage pulse [Figs. 2(d) and 2(e)] in all Fe islands and strip. Such a skyrmion lattice differs in their electronic structure between fcc and hcp Fe areas, giving rise to a signal contrast in the dI/dU map [Fig. 2(f)].

To investigate the mechanism behind such tip voltage-pulse-induced nonskyrmion-to-skyrmion phase transition, we conduct a detailed study of the pulse parameter, i.e., pulse voltage U and pulse duration time t . We first fix t to 50 ms and change U . Figures 3(a)–3(g) show a series of voltage pulses applied to the same location of an Fe island with an increasing amplitude from +1 to +6 V. This Fe island is originally in a nonskyrmion state with a mixture of the “bright” and the “dark” regions. The tip voltage pulse applied to the left corner of the island [red circle in Fig. 3(b)] changes the spatial arrangement of the electronic states, i.e., the “bright” and electronically more uniform phase is aggregated to the left corner. The boundary between the “bright” and the “dark” regions gradually shifts to right as the voltage increases, which can be considered as evidence of transition from the “dark” phase to the “bright” phase. The exact nature of the spin states of these phases are not known at this stage. At +6 V, a skyrmion lattice starts to appear within the “bright” region. We note that a similar phase evolution happens at the negative tip voltage pulses (see Appendix B). One can also fix U and change t . Figures 3(h)–3(p) show another series of voltage pulses applied to the same location of a different Fe island in which one fixes U to +5 V and varies t from 10 to 90 ms. Similar to Figs. 3(a)–3(g), the applied voltage pulse can change the texture of the electronic states by forming a more uniform “bright” region near the voltage-pulse location. However, the nonskyrmion-to-skyrmion phase transition does not happen until the

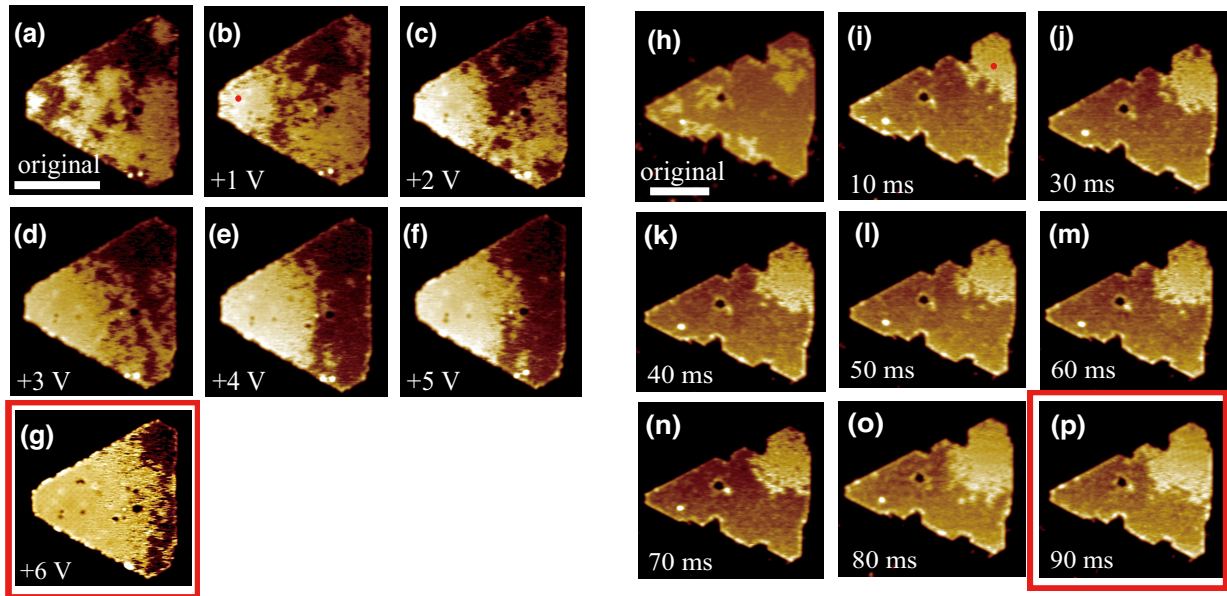


FIG. 3. (a)–(g) A series of SPSTM constant-current images of an Fe island under positive tip voltage pulses with a fixed 50-ms duration time but an increasing amplitude as denoted in the lower-left corner of the image. $U = 100$ mV, $I = 200$ pA for all and the scale bar is 10 nm. (h)–(p) A series of SPSTM constant-current images of an Fe island under tip voltage pulses with a fixed +5-V amplitude but an increasing duration time as denoted in the lower-left corner of the image. $U = 100$ mV, $I = 100$ pA for all and the scale bar is 10 nm.

duration time t exceeds 90 ms. We try different combinations of U and t whose results are summarized in Fig. 4. One marks the nonskyrmion-to-skyrmion phase transition boundary in this (U, t) phase diagram. Intriguingly, there is an inverse correlation between the threshold value of U and t .

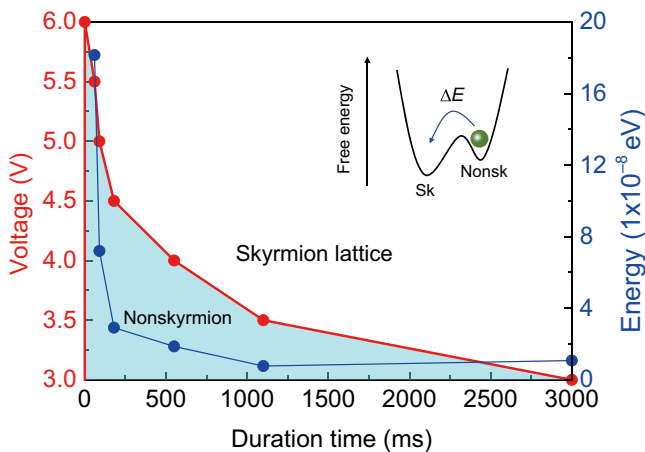


FIG. 4. The tip voltage-pulse-induced nonskyrmion to skyrmion phase transition as a function of pulse amplitude U and pulse duration time t . The estimated total injected energy for the phase transition is also plotted. Shown in the inset is the free-energy profile of different spin states in Fe/Ir(111) system.

Now we discuss the kinetic nature of the tip voltage-pulse-induced nonskyrmion-to-skyrmion phase transition. The tip voltage pulse yields both a large current density (on the order of 10^2 A/cm²) and a large electric field (on the order of 0.5 V/Å). Both the current and the electric field can drive the nonskyrmion to the skyrmion phase transition. In the former case (i.e., current), the spin-transfer torque (STT) from the spin-polarized current is often discussed [27]. However, the fact that the phase transition occurs under both positive and negative voltage pulses in a very similar manner implies that STT is unlikely responsible for the phase transition because STT depends on the spin polarization of the tunnel current and its direction. In the latter case (i.e., electric field), the electric field can cause a structural relaxation of the Fe atom as reported in the Fe/Cu(111) system [28]. This can affect the magnetic exchange interactions. The DMI can also be affected because it stems from the inversion symmetry breaking at the buried Fe/Ir interface (Rashba DMI) and is therefore sensitive to the vertical electric field applied by the tip. However, such an electric field will decay strongly with the distance from the surface due to the screening effect from the metallic Fe layer. The change of DMI is thus very limited. In our experiment, the inverse correlation between pulse parameter U and t strongly indicates that it is the total injected energy ΔE that triggers the nonskyrmion-to-skyrmion phase transition. ΔE is carried out by the tunneling electrons and can be roughly

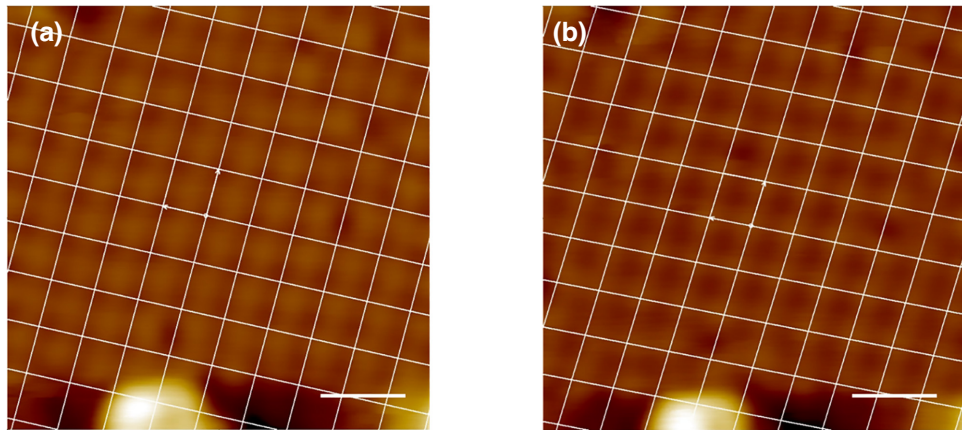


FIG. 5. (a),(b) SPSTM constant-current images under $+0.25$ and -0.25 T magnetic field, respectively. $U = 50$ mV, $I = 100$ pA for these images. The scale bar is 2 nm.

estimated by $\Delta E = |eU|It$. We plot such ΔE in Fig. 4. ΔE is drastically reduced as t increases and approaches a constant level (approximately 1×10^{-8} eV) when t exceeds 500 ms. This behavior strongly suggests that, in addition to ΔE , other factors should be considered especially for a very short tip pulse. Nevertheless, ΔE still plays a big role. To understand why there exists an energy threshold, one draws a free-energy profile in the inset of Fig. 4. As mentioned above, the delicate balance between different competing magnetic interactions in the Fe/Ir(111) system determines its magnetic ground state. The system could be easily trapped in many metastable spin states with close energy levels, such as the “bright” and the “dark” non-skyrmion phases. The skyrmion phase is the true magnetic ground state of the system with the lowest free energy. However, an energy barrier exists between them preventing the system from reaching its ground state. The applied voltage pulse supplies the required energy ΔE to overcome the barrier and drive the system into its ground state. We note that such tip voltage-pulse-induced nonskyrmion-to-skyrmion phase transition is irreversible (see Appendix C). Once the skyrmion phase is formed, it remains unchanged upon further applications of voltage pulses indicating that such a ground state is very stable. Actually, this skyrmion phase in the Fe monolayer on Ir(111) can sustain under an external field of up to $+9$ T [2].

The fact that the nonskyrmion-to-skyrmion phase transition is determined by the total injected energy is also consistent with a Joule heating picture, i.e., the system is thermally activated by the tunneling current. On the other hand, the locality of the phase transition as demonstrated in Figs. 1(c)–1(f) indicates the key role of a local electric field. Therefore, it appears that the transition is driven by a combination of electric field and Joule heating. Previous studies of nucleation and annihilation of magnetic skyrmion in the Pd/Fe bilayer on the Ir(111) system

propose an electric-field-assisted thermal-activation process in which the thermal energy barrier is electric field dependent [24,29]. We believe a similar mechanism is responsible for our experimental observations.

III. CONCLUSION

In summary, we observe various spin states in the as-grown Fe monolayer islands on Ir(111). A tip voltage pulse can be used to trigger a nonskyrmion-to-skyrmion phase transition. Such a transition is irreversible, indicating skyrmion as a true magnetic ground state in the system. We further demonstrate that this transition is determined by the total injected energy carried by the tunneling current. This finding adds more evidence of the feasibility of manipulating magnetic skyrmions on the nanometer scale via an electric manner.

ACKNOWLEDGMENT

This work is supported by National Key Research Program of China (Grant No. 2022YFA1403300), the National Natural Science Foundation of China (Grants No. 11427902, No. 11991060, No. 12074075, No. 12074080, and No. 12274088), the Shanghai Municipal Science and Technology Major Project (Grant No. 2019SHZDZX01), and the Shanghai Municipal Natural Science Foundation (Grant No. 20501130600, No. 22ZR1408100, and No. 22ZR1407400).

APPENDIX A: MAGNETIC ORIGIN OF THE SIGNAL CONTRAST FOR THE SQUARE LATTICE

In the SPSTM experiment, the spin-polarized tunneling current depends on the relative orientation between the tip and the local sample magnetization, giving rise to a signal contrast of magnetic nanoskyrmion in the constant-current

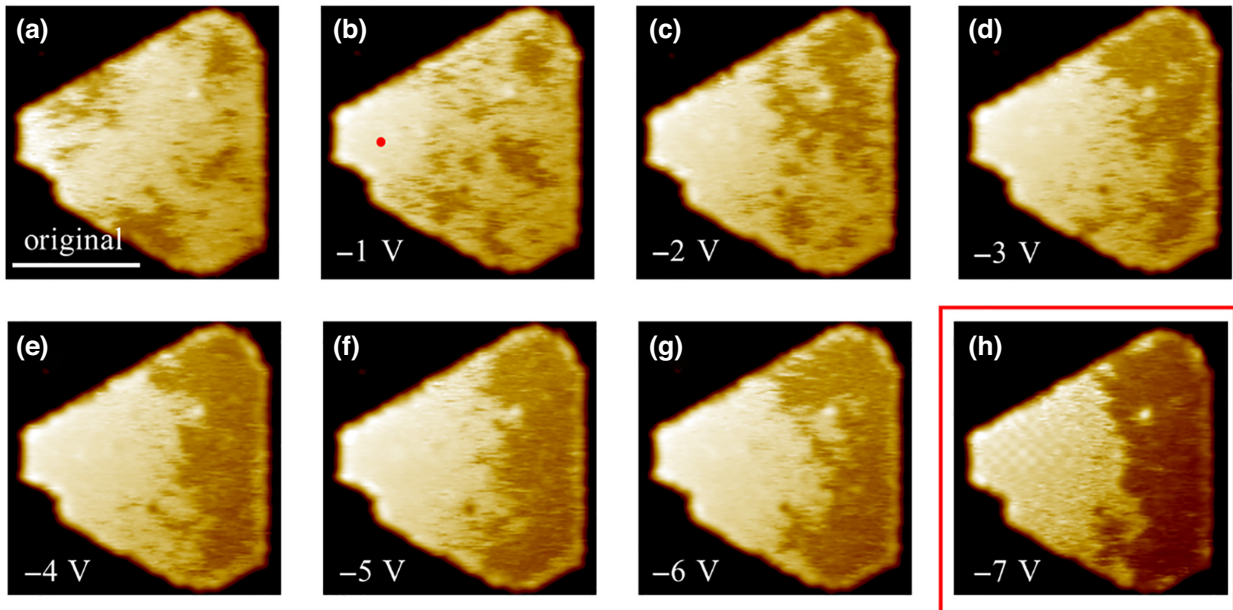


FIG. 6. (a)–(h) A series of SPSTM constant-current images of an Fe island under negative tip voltage pulses with a fixed 50-ms duration time but an increasing amplitude as denoted in the lower-left corner of the image. $U = 100$ mV, $I = 200$ pA for all and the scale bar is 10 nm.

STM image. To demonstrate it in our SPSTM measurement, one shows two constant-current STM images of the square lattice (presumably skyrmion) collected under the +0.25 T and -0.25 T magnetic field in Figs. 5(a) and 5(b), respectively. The applied magnetic field is big enough to flip the magnetic direction of the ferromagnetic Fe tip but not enough to change the skyrmion spin structure. As expected, the signal contrast of such a square lattice is reversed between Figs. 5(a) and 5(b), confirming its magnetic origin.

APPENDIX B: NEGATIVE TIP VOLTAGE-PULSE-INDUCED PHASE TRANSITION

One shows the tip voltage-pulse-induced nonskyrmion to skyrmion phase transition at the negative side. Similar to the positive case, a phase transition from the “dark” phase

to the “bright” phase happens at a lower voltage pulse. The nonskyrmion to skyrmion phase transition happens at -7 V (Fig. 6).

APPENDIX C: THE IRREVERSIBILITY OF NONSKYRMION TO SKYRMION PHASE TRANSITION

Figure 7 shows SPSTM constant-current images of an Fe island, which undergoes two consecutive tip voltage pulses. Although a tip voltage pulse can trigger a nonskyrmion to skyrmion phase transition, its reversed process will not happen. In other words, once the skyrmion phase is formed, it remains unchanged upon further applications of voltage pulses. Such irreversibility indicates that the skyrmion lattice is a true magnetic ground state of the Fe/Ir(111) system.

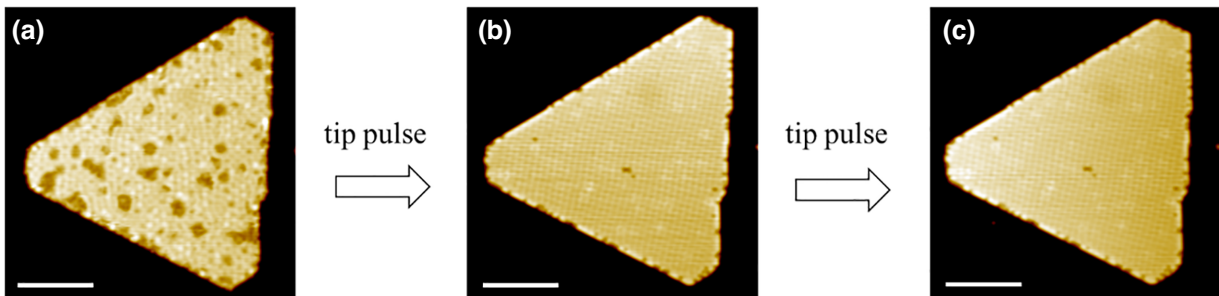


FIG. 7. (a)–(c) SPSTM constant-current images of an Fe island under two consecutive tip voltage pulses. $U = 50$ mV, $I = 100$ pA for all and the scale bar is 10 nm.

- [1] C. A. F. Vaz, J. A. C. Bland, and G. Lauhoff, Magnetism in ultrathin film structures, *Rep. Prog. Phys.* **71**, 056501 (2008).
- [2] K. von Bergmann, A. Kubetzka, O. Pietzsch, and R. Wiesendanger, Interface-induced chiral domain walls, spin spirals and skyrmions revealed by spin-polarized scanning tunneling microscopy, *J. Phys.: Condens. Matter* **26**, 394002 (2014).
- [3] I. Dzyaloshinsky, A thermodynamic theory of “weak” ferromagnetism of antiferromagnetics, *J. Phys. Chem. Solids* **4**, 241 (1958).
- [4] T. Moriya, Anisotropic superexchange interaction and weak ferromagnetism, *Phys. Rev.* **120**, 91 (1960).
- [5] M. Bode, M. Heide, K. von Bergmann, P. Ferriani, S. Heinze, G. Bihlmayer, A. Kubetzka, O. Pietzsch, S. Blügel, and R. Wiesendanger, Chiral magnetic order at surfaces driven by inversion asymmetry, *Nature* **447**, 190 (2007).
- [6] P. Ferriani, K. von Bergmann, E. Y. Vedmedenko, S. Heinze, M. Bode, M. Heide, G. Bihlmayer, S. Blügel, and R. Wiesendanger, Atomic-Scale Spin Spiral with a Unique Rotational Sense: Mn Monolayer on W(001), *Phys. Rev. Lett.* **101**, 027201 (2008).
- [7] K. Von Bergmann, S. Heinze, M. Bode, E. Y. Vedmedenko, G. Bihlmayer, S. Blugel, and R. Wiesendanger, Observation of a complex nanoscale magnetic structure in a hexagonal Fe monolayer, *Phys. Rev. Lett.* **96**, 167203 (2006).
- [8] K. von Bergmann, S. Heinze, M. Bode, G. Bihlmayer, S. Blugel, and R. Wiesendanger, Complex magnetism of the Fe monolayer on Ir(111), *New J. Phys.* **9**, 396 (2007).
- [9] S. Heinze, K. von Bergmann, M. Menzel, J. Brede, A. Kubetzka, R. Wiesendanger, G. Bihlmayer, and S. Blugel, Spontaneous atomic-scale magnetic skyrmion lattice in two dimensions, *Nat. Phys.* **7**, 713 (2011).
- [10] J. Grenz, A. Kohler, A. Schwarz, and R. Wiesendanger, Probing the Nano-Skyrmion Lattice on Fe/Ir(111) with Magnetic Exchange Force Microscopy, *Phys. Rev. Lett.* **119**, 047205 (2017).
- [11] J. Hagemeister, D. Iaia, E. Y. Vedmedenko, K. von Bergmann, A. Kubetzka, and R. Wiesendanger, Skyrmions at the Edge: Confinement Effects in Fe/Ir(111), *Phys. Rev. Lett.* **117**, 207202 (2016).
- [12] A. Sonntag, J. Hermenau, S. Krause, and R. Wiesendanger, Thermal Stability of an Interface-Stabilized Skyrmion Lattice, *Phys. Rev. Lett.* **113**, 077202 (2014).
- [13] P. J. Hsu, A. Finco, L. Schmidt, A. Kubetzka, K. von Bergmann, and R. Wiesendanger, Guiding Spin Spirals by Local Uniaxial Strain Relief, *Phys. Rev. Lett.* **116**, 017201 (2016).
- [14] P.-J. Hsu, A. Kubetzka, A. Finco, N. Romming, K. von Bergmann, and R. Wiesendanger, Electric-field-driven switching of individual magnetic skyrmions, *Nat. Nanotechnol.* **12**, 123 (2017).
- [15] M. Shuai, Y. Yang, H. Huang, R. Song, Y. Zhu, Y. Liao, Y. Zhu, X. Zhou, L. Yin, and J. Shen, The influence of adatom diffusion on the formation of skyrmion lattice in sub-monolayer Fe on Ir(111), *Vacuum* **212**, 112071 (2023).
- [16] S. Woo, K. Litzius, B. Kruger, M. Y. Im, L. Caretta, K. Richter, M. Mann, A. Krone, R. M. Reeve, M. Weigand, P. Agrawal, I. Lemesh, M. A. Mawass, P. Fischer, M. Klau, and G. R. S. D. Beach, Observation of room-temperature magnetic skyrmions and their current-driven dynamics in ultrathin metallic ferromagnets, *Nat. Mater.* **15**, 501 (2016).
- [17] W. Jiang, X. Zhang, G. Yu, W. Zhang, X. Wang, M. Benjamin Jungfleisch, John E. Pearson, X. Cheng, O. Heinonen, K. L. Wang, Y. Zhou, A. Hoffmann, and Suzanne G. E. te Velthuis, Direct observation of the skyrmion Hall effect, *Nat. Phys.* **13**, 162 (2017).
- [18] M. Schott, A. Bernand-Mantel, L. Ranno, S. Pizzini, J. Vogel, H. Béa, C. Baraduc, S. Auffret, G. Gaudin, and D. Givord, The skyrmion switch: Turning magnetic skyrmion bubbles on and off with an electric field, *Nano Lett.* **17**, 3006 (2017).
- [19] P. Huang, M. Cantoni, A. Kruchkov, J. Rajeswari, A. Magrez, F. Carbone, and H. M. Rønnow, In situ electric field skyrmion creation in magnetoelectric Cu₂OSeO₃, *Nano Lett.* **18**, 5167 (2018).
- [20] T. Srivastava, M. Schott, R. Juge, V. Křížáková, M. Belmeguenai, Y. Roussigné, A. Bernand-Mantel, L. Ranno, S. Pizzini, S.-M. Chérif, A. Stashkevich, S. Auffret, O. Boulle, G. Gaudin, M. Chshiev, C. Baraduc, and H. Béa, Large-voltage tuning of Dzyaloshinskii–Moriya interactions: A route toward dynamic control of skyrmion chirality, *Nano Lett.* **18**, 4871 (2018).
- [21] Y. Wang, L. Wang, J. Xia, Z. Lai, G. Tian, X. Zhang, Z. Hou, X. Gao, W. Mi, C. Feng, M. Zeng, G. Zhou, G. Yu, G. Wu, Y. Zhou, W. Wang, X.-x. Zhang, and J. Liu, Electric-field-driven non-volatile multi-state switching of individual skyrmions in a multiferroic heterostructure, *Nat. Commun.* **11**, 3577 (2020).
- [22] Y. Ba, S. Zhuang, Y. Zhang, Y. Wang, Y. Gao, H. Zhou, M. Chen, W. Sun, Q. Liu, G. Chai, J. Ma, Y. Zhang, H. Tian, H. Du, W. Jiang, C. Nan, J.-M. Hu, and Y. Zhao, Electric-field control of skyrmions in multiferroic heterostructure via magnetoelectric coupling, *Nat. Commun.* **12**, 322 (2021).
- [23] N. Romming, C. Hanneken, M. Menzel, J. E. Bickel, B. Wolter, K. von Bergmann, A. Kubetzka, and R. Wiesendanger, Writing and deleting single magnetic skyrmions, *Science* **341**, 636 (2013).
- [24] F. Muckel, S. von Malottki, C. Holl, B. Pestka, M. Pratzer, P. F. Bessarab, S. Heinze, and M. Morgenstern, Experimental identification of two distinct skyrmion collapse mechanisms, *Nat. Phys.* **17**, 395 (2021).
- [25] R. Wiesendanger, Spin mapping at the nanoscale and atomic scale, *Rev. Mod. Phys.* **81**, 1495 (2009).
- [26] K. von Bergmann, M. Menzel, A. Kubetzka, and R. Wiesendanger, Influence of the local atom configuration on a hexagonal skyrmion lattice, *Nano Lett.* **15**, 3280 (2015).
- [27] X. Yu, D. Morikawa, Y. Tokunaga, M. Kubota, T. Kurumaji, H. Oike, M. Nakamura, F. Kagawa, Y. Taguchi, T.-h. Arima, M. Kawasaki, and Y. Tokura, Current-induced nucleation and annihilation of magnetic skyrmions at room temperature in a chiral magnet, *Adv. Mater.* **29**, 1606178 (2017).
- [28] L. Gerhard, T. K. Yamada, T. Balashov, A. F. Takács, R. J. H. Wesselink, M. Däne, M. Fechner, S. Ostanin, A. Ernst, I. Mertig, and W. Wulfhekel, Magnetoelectric coupling at metal surfaces, *Nat. Nanotechnol.* **5**, 792 (2010).
- [29] M. A. Goerzen, S. von Malottki, G. J. Kwiatkowski, P. F. Bessarab, and S. Heinze, Atomistic spin simulations of electric-field-assisted nucleation and annihilation of magnetic skyrmions in Pd/Fe/Ir(111), *Phys. Rev. B* **105**, 214435 (2022).